Supplementary Material

Phenytoin-like Antiepileptic Effect of Cannabidiol and Related Phytocannabinoid Metabolites: Structural Insights from Molecular Modeling

Experimental Methods

For structural input for calculations in general, the molecules were manually built based on conformations described earlier. For phenytoin (PHT), structural input used data from crystallo-graphic [1] and computational studies [2–10], while for the structure of the $\Delta^{2(E)}$-valproic acid derivative data from molecular modeling experiments were consulted [11,12]. For natural cannabidiol, that is (–)-(*R*,*R*)-CBD, crystallographic [13–15] and solution NMR experiments [16,17], as well as molecular modeling studies [16–22] provided guidance. Accordingly, the cyclohexene moiety of CBD assumes a half-chair conformation with the resorcinol group in a pseudo-equatorial and the isopropenyl group in an equatorial position; for calculations, the *n*-pentyl side chain in a fully extended conformation was chosen. Electrostatic potential maps (EPMs) projected onto the electron density surface of the energy minimized molecules were calculated by ωB97X-D/6-31G* density functional method using the C-PCM continuum solvation model (water) (Spartan'16 Version 2.0.7, Wavefunction, Inc., Irvine, CA, USA). The surfaces were color-coded according to the potential with electron rich regions colored red and electron poor regions colored blue. Figure 4 (main text) displays the molecules in similar orientation as derived from their overlays (as in Figure 3B in main text) by five tethered atom pairs of PHT and 7-COOH-CBD (atoms of the hydantoin imidic -CONH with -COOH of the CBD metabolite, and atoms of the pivot bond connecting the hydantoin and phenyl rings of PHT or the cyclohexenyl and aryl moieties of the cannabinoid).

Superpositions shown in Figures 3, 5 and 6 in the main text were done using Discovery Studio Visualizer 4.1 (Accelrys/BIOVIA, San Diego, CA, USA) software as follows. The molecules were manually built, and their energy minimized conformation was obtained using CHARMm molecular mechanics simulation. The optimized structures of the (*S*,*S*), (*S*,*R*), and (*R*,*S*) isomers of CBD were obtained in two steps: First, the terpenyl fragment with the desired configuration was built manually and its minimum energy conformation was calculated. In the second step, the appropriate isomer was joined with the olivetol fragment in the desired stereochemical arrangement and the minimum energy conformation of the full CBD structure was then calculated. Alignments of the molecules were done either by balanced (50:50) steric + electrostatic fields overlay or by selected atom–atom tethers according to command options in the Structure/Superimpose/Molecular Overlay menu of the software. Hydrogen atoms are omitted except where indicated. The energy minimized structures of the individual molecules in the orientation used for the relevant superpositions are shown in Figures S1-S5 of the ***Supplementary material*** (see below).

References for Experimental Methods in Supplementary material

1. Camerman A, Camerman N (1971) The stereochemical basis of anticonvulsant drug action. I. The crystal and molecular structure of diphenylhydantoin, a noncentrosymmetric structure solved by centric symbolic addition. Acta Cryst B27: 2205–2211.

2. Camerman A, Camerman N (1977) Ethylphenacemide and phenacemide: Conformational similarities to diphenylhydantoin and stereochemical basis of anticonvulsant activity. Proc Natl Acad Sci USA 74: 1264–1266.

3. Wong MG, Defina JA, Andrews PR (1986) Conformational analysis of clinically active anticonvulsant drugs. J Med Chem 29: 562–572.

4. Murray JS, Abu-Awwad F, Politzer P, Wilson LC, Troupin AS, Wall RE (1998) Molecular surface electrostatic potentials of anticonvulsant drugs. Int J Quant Chem 70: 1137–1143.

5. Lipkind GM, Fozzard HA (2010) Molecular model of anticonvulsant drug binding to the voltage-gated sodium channel inner pore. Mol Pharmacol 78: 631–638.

6. Khan HN, Kulsoom S, Rashid H (2012) Ligand based pharmacophore model development for the identification of novel antiepileptic compounds. Epilepsy Res 98: 62–71.

7. Trišović NP, Božić BD, Lović JD, Vitnik VD, Vitnik ŽJ, Petrović SD, Avramov Ivić ML (2015) Electrochemical characterization of phenytoin and its derivatives on bare gold electrode. Electrochim Acta 161: 378–387.

8. Luchian R, Vinţeler E, Chiş C, Vasilescu M, Leopold N, Chiş V (2017) Molecular structure of phenytoin: NMR, UV-Vis and quantum chemical calculations. Croat Chem Acta 88: 511–522.

9. Serdaroğlu G, Ortiz JV (2017) Ab initio calculations on some antiepileptic drugs such as phenytoin, phenbarbital, ethosuximide and carbamazepine. Struct Chem 28: 957–964.

10. Jones GL, Wimbish GH (1985) Hydantoins. In: Frey H-H, Janz D (eds.) Antiepileptic Drugs. Springer-Verlag: Berlin, pp. 351–419.

11. Tasso SM, Bruno-Blanch LE, Moon SC, Estiú GL (2000) Pharmacophore searching and QSAR analysis in the design of anticonvulsant drugs. J Mol Struct (Theochem) 504: 229–240.

12. Tasso SM, Moon SC, Bruno-Blanch LE, Estiú GL (2004) Characterization of the anticonvulsant profile of valproamide derivatives. Bioorg Med Chem 12: 3857–3869.

13. Jones PG, Falvello L, Kennard O, Sheldrick GM, Mechoulam R (1977) Cannabidiol. Acta Cryst B33: 3211–3214.

14. Ottersen T, Rosenqvist E, Turner CE, El-Feraly FS (1977) The crystal and molecular structure of cannabidiol. Acta Chem Scand B31: 807–812.

15. Mayr T, Grassl T, Korber N, Christoffel V, Bodensteiner M (2017) Cannabidiol revisited. IUCrData 2: x170276. doi: 10.1107/S2414314617002760.

16. Tamir I, Mechoulam R, Meyer AY (1980) Cannabidiol and phenytoin: a structural comparison. J Med Chem 23: 220–223.

17. Kane VV, Martin AR, Jaime C, Ōsawa E (1984) Dynamic nuclear magnetic resonance and empirical force field studies of cannabidiol. Tetrahedron 40: 2919–2927.

18. Reggio PH, Bramblett RD, Yuknavich H, Seltzman HH, Fleming DN, Fernando SR, Stevenson LA, Pertwee RG (1995) The design, synthesis and testing of desoxy-CBD: further evidence for a region of steric interference at the cannabinoid receptor. Life Sci 56: 2025–2032.

19. Borges RS, Batista J Jr, Viana RB, Baetas AC, Orestes E, Andrade MA, Honório KM, da Silva ABF (2013) Understanding the molecular aspects of tetrahydrocannabinol and cannabidiol as antioxidants. Molecules 18: 12663–12674.

20. Borges RS, da Silva ABF (2017) Cannabidiol as an antioxidant. In: Preedy VR (ed.) Handbook of Cannabis and Related Pathologies. Biology, Pharmacology, Diagnosis, and Treatment. Elsevier, Inc.: London, pp. e122–e130.

21. Berber H, Lameiras P, Denhez C, Antheaume C, Clayden J (2014) Atropisomerism about aryl–Csp3 bonds: the electronic and steric influence of *ortho*-substituents on conformational exchange in cannabidiol and linderatin derivatives. J Org Chem 79: 6015–6027.

22. Kozela E, Haj C, Hanuš L, Chourasia M, Shurki A, Juknat A, Kaushansky N, Mechoulam R, Vogel Z (2016) HU-446 and HU-465, derivatives of the non-psychoactive cannabinoid cannabidiol, decrease the activation of encephalitogenic T cells. Chem Biol Drug Des 87: 143–153.

Supplementary Table

Chemical structure, short name and SMILES notation of compounds specifically mentioned in the text

Structure	*Short name*	*SMILES notation*
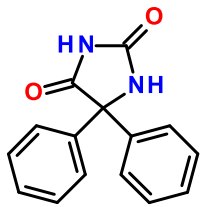	Phenytoin (PHT)	O=C1NC(=O)C(N1)(c2ccccc2)c3ccccc3
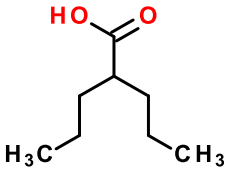	Valproic acid	CCCC(CCC)C(=O)O
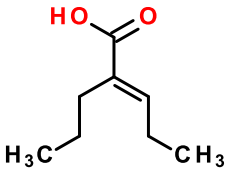	$\Delta^{2(E)}$-Valproic acid	CCC\C(=C/CC)\C(=O)O
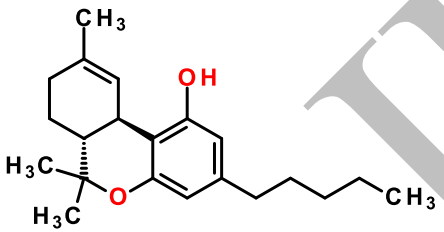	Δ^{9}-THC	CCCCCc1cc(O)c2[C@@H]3C=C(C)CC[C@H]3C(C)(C)Oc2c1

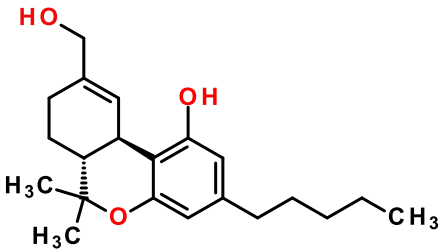	11-OH-THC	CCCCCc1cc(O)c2[C@@H]3C=C(CO)CC[C@H]3C(C)(C)Oc2c1
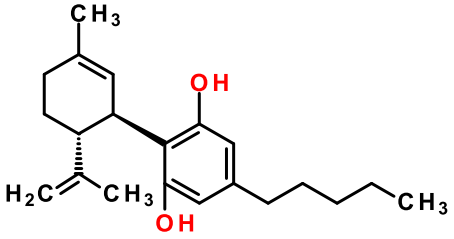	CBD	CCCCCc1cc(O)c([C@@H]2C=C(C)CC[C@H]2C(=C)C)c(O)c1
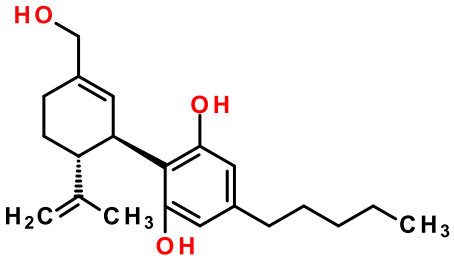	7-OH-CBD	CCCCCc1cc(O)c([C@@H]2C=C(CO)CC[C@H]2C(=C)C)c(O)c1
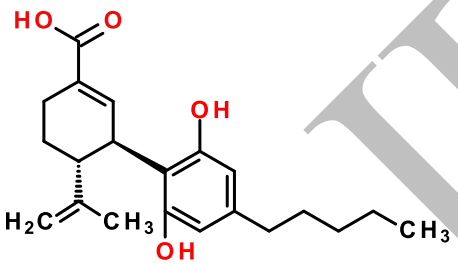	7-COOH-CBD	CCCCCc1cc(O)c([C@@H]2C=C(CC[C@H]2C(=C)C)C(=O)O)c(O)c1

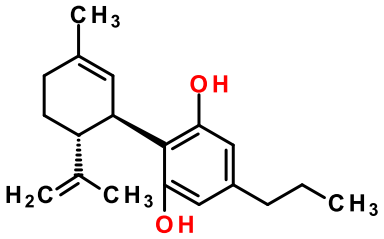	CBDV	CC(=C)[C@@H]2CCC(C)=C[C@H]2c1c(O)cc(CCC)cc1O
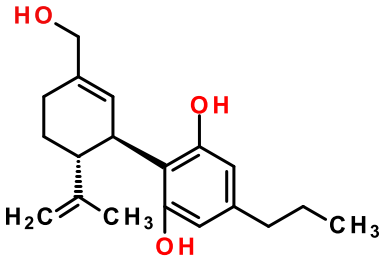	7-OH-CBDV	CCCc1cc(O)c([C@@H]2C=C(CO)CC[C@H]2C(=C)C)c(O)c1
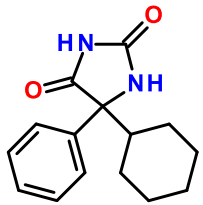	Cyclohexyl-PHT analogue	O=C1NC(=O)C(N1)(C2CCCCC2)c3ccccc3
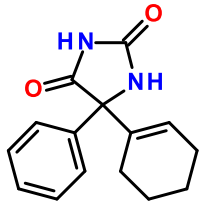	5-Cyclohexenyl-PHT analogue	O=C1NC(=O)C(N1)(C2=CCCCC2)c3ccccc3

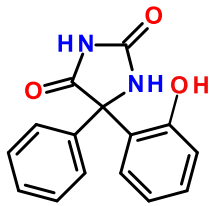	2’-OH-PHT	Oc1ccccc1C2(NC(=O)NC2=O)c3ccccc3
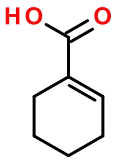	Cyclohex-1-ene–carboxylic acid	OC(=O)C1=CCCCC1
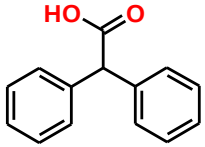	Diphenylacetic acid	OC(=O)C(c1ccccc1)c2ccccc2
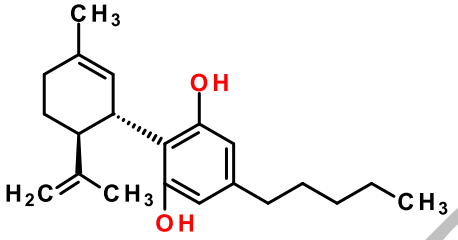	(*S*,*S*)-CBD	CCCCCc1cc(O)c([C@H]2C=C(C)CC[C@@H]2C(=C)C)c(O)c1
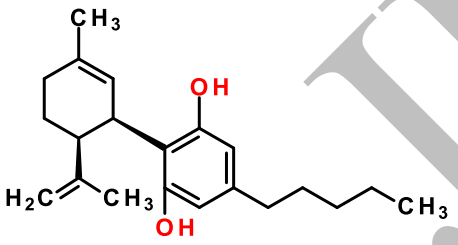	(*R*,*S*)-CBD	CCCCCc1cc(O)c([C@@H]2C=C(C)CC[C@@H]2C(=C)C)c(O)c1

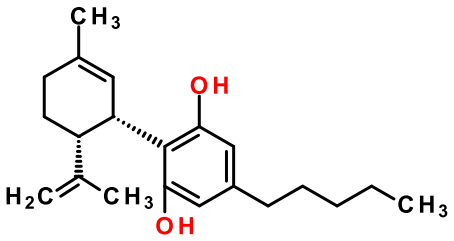	(*S*,*R*)-CBD	CCCCCc1cc(O)c([C@H]2C=C(C)CC[C@H]2C(=C)C)c(O)c1

Supplementary Figures

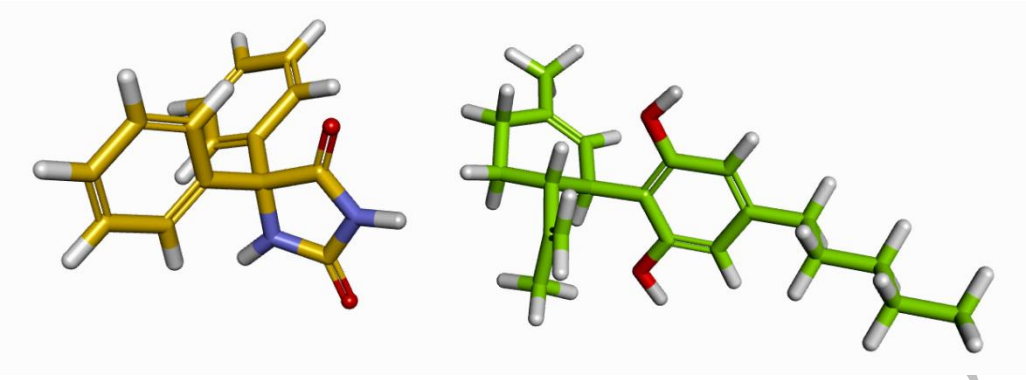

Figure S1. Energy-minimized structures of phenytoin (PHT; gold carbon atoms) and CBD (green carbon atoms) in the orientation proposed by Tamir *et al.* (Ref. 16 in *Supplementary material* and Ref. 56 in main text). For superposition, see figure 3A in main text.

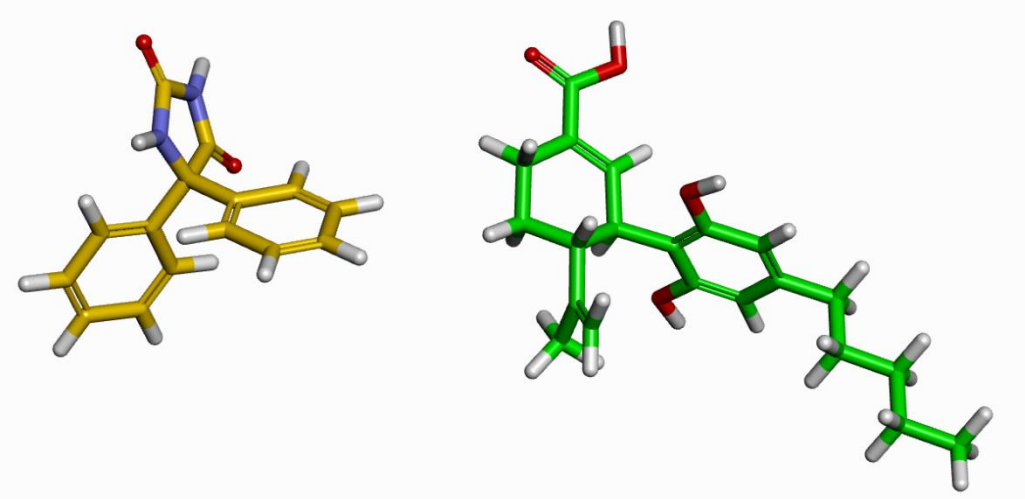

Figure S2. Energy-minimized structures of PHT (gold carbon atoms) and 7-COOH-CBD (green carbon atoms) in the orientation proposed in this study. For superposition, see figure 3B in main text.

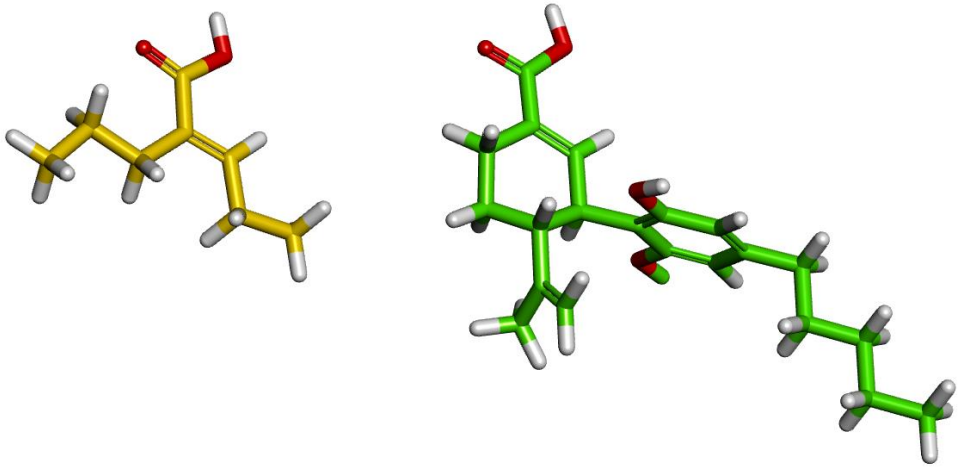

Figure S3. Energy-minimized structures of $\Delta^{2(E)}$-valproic acid (gold carbon atoms) and CBD (green carbon atoms). For superposition, see figure 5 in main text.

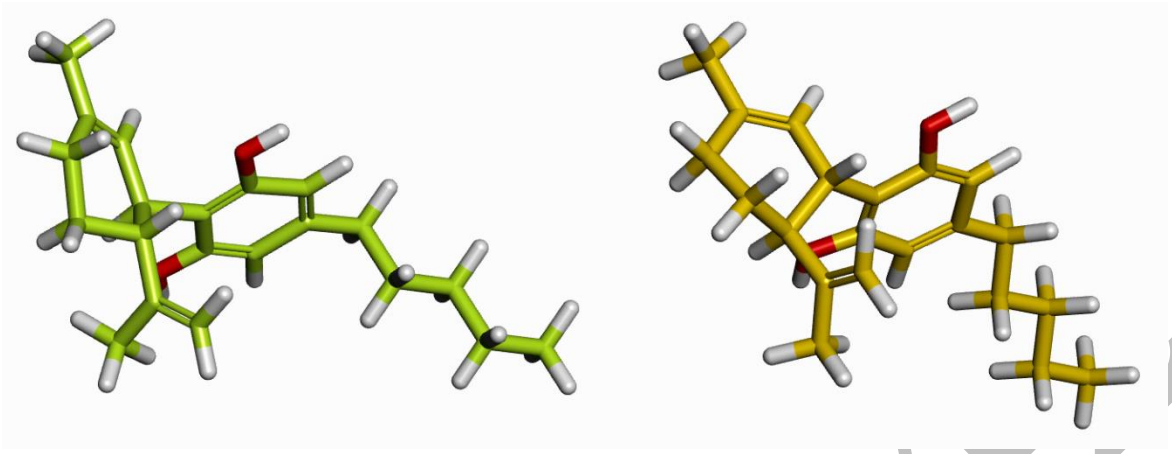

Figure S4. Energy-minimized structures of (*R*,*R*)-CBD (green carbon atoms) and (*S*,*S*)-CBD (gold carbon atoms). Note that the isopropenyl moiety is in pseudo-equatorial position in both isomers. For superposition, see figure 6 in main text.

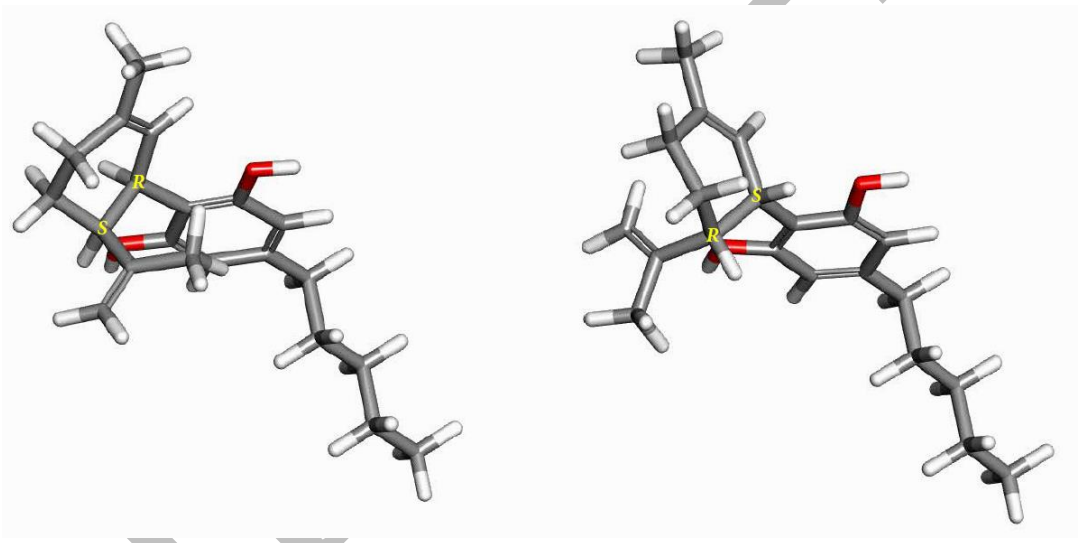

Figure S5. Energy-minimized structures of (*R*,*S*)-CBD (left) and (*S*,*R*)-CBD (right).